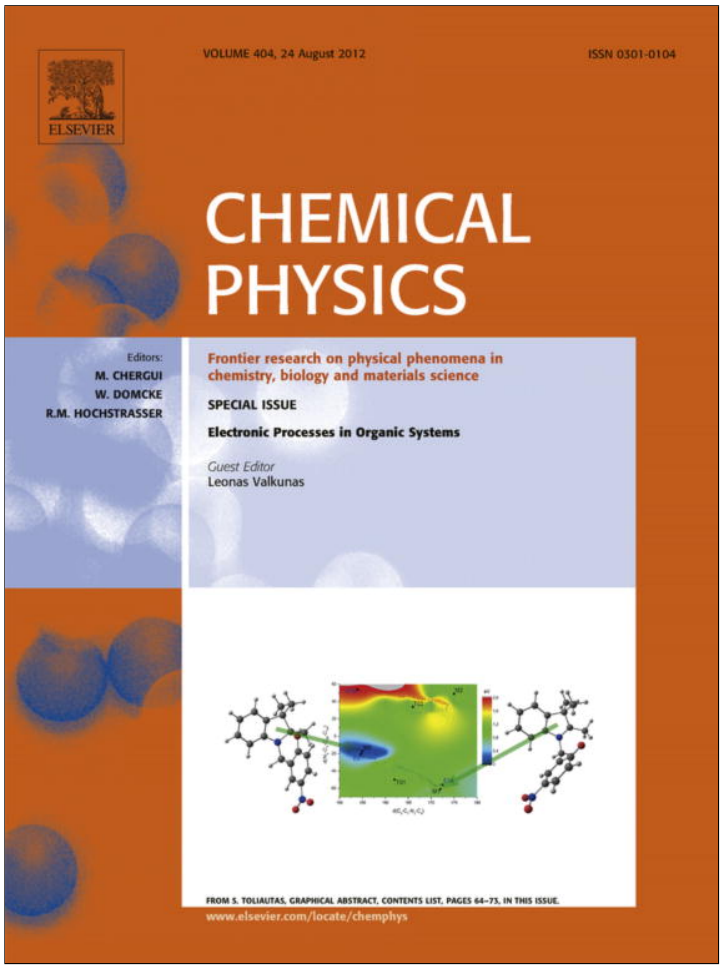

Chemical Physics 404 (2012) 88–93

Contents lists available at SciVerse ScienceDirect

Chemical Physics

journal homepage: www.elsevier.com/locate/chemphys

Analysis of the carrier transport in molecularly doped polymers using the multiple trapping model with the Gaussian trap distribution

Andrey Tyutnev *, Renat Ikhsanov, Vladimir Saenko, Evgenii Pozhidaev

National Research University Higher School of Economics, 20 Myasnitskaya Ulitsa, Moscow 101000, Russia

ARTICLE INFO

Article history:
Available online 25 April 2012

Keywords:
Transient curves
Current universality
Poole–Frenkel effect
Numerical computations

ABSTRACT

We have performed the comprehensive analysis of the time of flight curves using the multiple trapping model with the Gaussian trap distribution. Our analysis shows that flat plateaus on the computed curves are rare events. We have shown numerically that plateau formation for the non-equilibrium transport may be due to the presence of a thin defective (depletion) layer on the sample surface (two-layer model of a polymer film). Also, to describe the Poole–Frenkel effect, we have explicitly introduced an analogous field dependence for the frequency factor.

1. Introduction

Modern optoelectronic devices such as light-emitting diodes [1], field-effect transistors [2] and solar cells [3] using organic semiconductors require profound understanding of the charge carrier transport for their efficient operation similar to that already achieved in the electrophotographic technology [4,5]. In a recently published review [6], the problem of the charge carrier transport in organic semiconductors has been discussed in detail. It shows that the Gaussian disorder model (GDM) based on a hopping transport of charge carriers still remains a powerful instrument for describing charge motion in disordered organic substances (small molecule glasses, molecularly doped polymers, polymers with charge-transporting molecules residing in the main chain or as pendant groups) [7,8].

As most device-operation oriented calculations refer to steady-state conditions [1–3], they mostly rely on the well-known empirical expressions for carrier mobilities at different fields and temperatures derived from computer (mainly Monte-Carlo) simulations based on the GDM for a model disordered organic semiconductor [4,8].

Experimental studies of the charge carrier transport employ the famous time of flight (TOF) technique, which allows not only to measure the carrier mobility but to study the non-equilibrium phase of the transport process by observing TOF current transients on a wide time scale following a δ-pulse excitation. Based on the optical TOF technique, these transients have been shown to consist of an initial spike transforming into a flat or slightly sloping plateau followed by an anomalously long tail (when plotted in linear $j - t$ coordinates) and seemingly agree with the GDM predictions [4].

To supplement the model Monte-Carlo simulations, we developed a numerical program for a quasi-band analog of the GDM, the so-called multiple trapping model with the Gaussian trap distribution (MTMg) [9,10]. Both approaches give close results as far as TOF shapes are concerned. One of the factors, which stimulated this theoretical effort, is the much-changed situation in the carrier transport after we introduced an electron gun to perform TOF measurements in the widest dynamic range realizing all three modifications of the TOF experiment [11]. These are the conventional TOF method with the surface generation, the TOF-2 technique with the bulk generation and a TOF-1a variant in which the width of the generation zone varies in a controlled manner.

It has been revealed that the carrier transport in a typical polar MDP is non- equilibrium despite the fact that TOF curves feature a flat plateau [9–11]. Also, it was shown that cusps (rising plateaus), traditionally disregarded by investigators [4], reflected some internal property of a MDP sample. To explain the whole plethora of these new observations, a two-layer multiple trapping model for universal current transients in MDPs has been developed [12]. Its general features are as follows.

Real MDP sample is represented by a two-layer structure consisting of a thin surface layer (about 1 μm thick) and a polymer itself. The mobility of charge carriers in the surface layer is several times lower than in the bulk as a result of increased trap concentration in it. It is important that the same exponential MTM (except trap concentrations) apply to both regions. The origin of traps remained obscure but this two-layer model allowed explaining experimental observations previously viewed as contradictory [13,14].

* Corresponding author.
E-mail address: aptyutnev@yandex.ru (A. Tyutnev).

0301-0104/$ - see front matter Crown Copyright © 2012 Published by Elsevier B.V. All rights reserved.
http://dx.doi.org/10.1016/j.chemphys.2012.03.004

An exponential trap distribution with a rather large dispersion parameter (close to 0.8) describes a dispersive carrier transport. Then, TOF-2 curves, obviously unaffected by the surface layer (bulk excitation), should have a non-Gaussian form in accordance with experiment. Transient curves produced by 3 keV electrons (maximum range about 0.3 μm) feature pronounced cusps as carriers exit generation zone in the defective layer and enter the bulk where their mobility is several times higher. As electron energy increases, the fraction of carriers generated in the bulk increases leading to the formation of the progressively weaker cusps. At some electron energy a perfectly flat plateau appears as a result of fine tuning of two currents, one being due to carriers generated in the surface layer, the other arising from bulk generated carriers. At still higher energies, the plateau begins to slope, until finally, the bulk excitation makes the current form featureless when viewed in linear coordinates. It is important to stress that in all cases, whatever the form of the plateau (flat one included), the tail stays anomalously broad, reflecting dispersive rather than the Gaussian carrier transport. The two-layer model is capable of semiquantitatively describing the whole sequence of the current shape changes [12]. Surely, the above model captures truthfully the physics of the flat plateau formation arising from an intricate interplay of carriers emerging from the surface layer and the bulk.

In the present paper we compute TOF current transients for a homogeneous polymer using MTMg for several values of the disorder energy σ, an electric field and temperature. Then we introduce a two-layer model based on the MTMg aiming to explain TOF-1a results using model parameters for a typical MDP.

2. Homogeneous polymer

In our computations we rely on reported values of the GDM parameters extracted using the dipolar disorder formalism of Borsenberger and Bässler [8,15]. These are the total disorder energy σ, the mobility of carriers μ_0 extrapolated to zero electric field (via Poole–Frenkel functional dependence) for temperature $T \to \infty$ and the mean distance ρ between dopant molecules calculated using the lattice gas model ($\rho = N_d^{-1/3}$ where N_d is the dopant concentration).

The simple relationship between μ_0 and ρ [16] (notations are standard)

$$\mu_0 = \frac{e}{kT}\rho^2 \nu_{hh} \tag{1}$$

allows one to define frequency ν_{hh} which may be related to the zero-field frequency factor ν_{00} of the model ($\nu_{00} = 6\nu_{hh}$ [9]). MTMg parameters σ and μ_0 are taken to be the same as given above. The last parameter of the model, the lifetime of the quasi-free carriers τ_0, is found from the relationship $\nu_{00}\tau_0 = 3.0$ [9]. The situation with a finite electric field is discussed later.

Parameter values chosen for numerical simulations are as follows: $\mu_0 = 0.01$ cm^2/V s, $\sigma = 0.13$ eV and $\nu_{00} = 10^{11}$ c^{-1} and are close to those for polycarbonate doped with 30 wt.% of aromatic hydrazone DEH (30%DEH:PC) [9,17]. In addition, the sample thickness L is 20 μm, the electric field $F = 20$ V/μm, temperature 290 K ($kT = 0.025$ eV) and the planar density of the generated carriers 10^8 cm^{-2} (a small signal regime). When these change, it is clearly stated.

We start our analysis by investigating effects of the total disorder σ (Fig. 1). Current curves coincide at early times ($\leqslant 10$ fs), then they start to diverge, their decay generally following an algebraic law $j \propto t^{-\beta}$. The exponent $\beta = -\frac{d\lg j}{d\lg t}$ depends on time and progressively diminishes until a kink occurs signaling carrier transit across the sample. Two tangents (dotted straight lines) on a $\lg t - \lg j$ plot just preceding and following the kink intersect at the transit time t_{tr} (shown on the figure for curve 3). Also, the slopes of these tangents

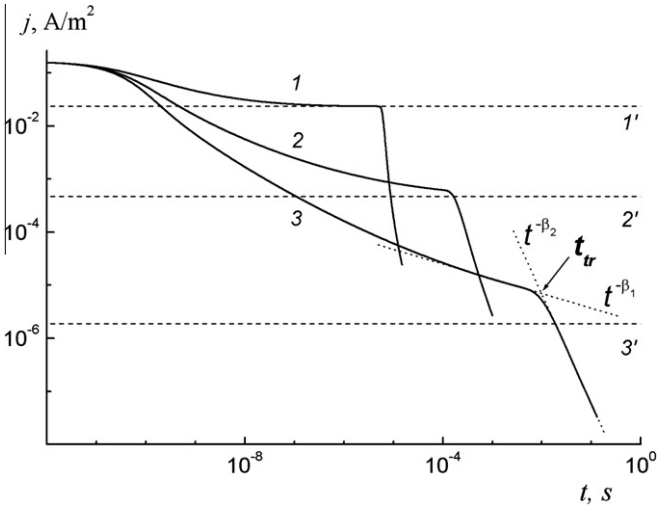

Fig. 1. Computed TOF transients (solid curves) in logarithmic coordinates. Parameter σ equals 0.07 (*1*), 0.1 (*2*) and 0.13 eV (*3*). Dashed straight lines refer to a semi-infinite sample and belong to the corresponding solid curve. The procedure to find t_{tr} is illustrated for curve *3*.

β_1 (before) and β_2 (after the transit) are useful characteristics of the carrier transport. Values of these parameters are summarized in Table 1. We see that as σ rises t_{tr} and β_1 both increase (especially strongly the first one) but β_2 systematically decreases.

It is known that MTMg predicts mobility equilibration at long times. Dashed straight lines on the figure show the equilibrium currents in a semi-infinite sample. Also, note that TOF curves *2* and *3* are similar to dispersive transients if viewed at times bracketing the time of flight ($10^{-2}t_{tr} \leqslant t \leqslant 10^2 t_{tr}$) but the famous criterion of the Scher–Montroll theory [18] or the MTM [11] ($\beta_1 + \beta_2 = 2.0$) fails.

Fig. 2 gives the above curves in a linear $j - t$ representation in a normalized form. Traditionally found two times of flight (t_0 and $t_{1/2}$ shown for curve *2*) and the relative tail width $W = \frac{t_{1/2} - t_0}{t_{1/2}}$ are also included in Table 1. While for curves *1* and *2* this procedure is rather straightforward, finding this data for the last curve is hardly possible. Still, according to the traditional classification only two first curves may be qualified as non-dispersive (in a sense that they can be readily processed in linear coordinates) whereas the last one should definitely be regarded as a dispersive one. Note that the point with coordinates (1, 1) on the figure corresponds to the intersection of the two tangents mentioned above.

Unlike curves *2* and *3*, which are non-equilibrium, curve *1* (see Figs. 1 and 2) is unique as it is characterized by a flat plateau. This feature is certainly due to the low value of σ. Experiment fully corroborates this conclusion: TAPC glass ($\sigma = 0.067$ eV) and TAPC doped polystyrene at high loadings ($\sigma \leqslant 0.075$ eV) [19,20] exhibit flat plateaus with times of flight in the microsecond range in full accord with our computations.

It is known that the GDM (and even more so the MTMg) is incapable of explaining consistently the origin of the Poole–Frenkel

Table 1
Computed slopes and times of flight for three values of σ.

Parameter	σ, eV		
	0.07	0.10	0.13
β_1	$\leqslant$0.03	0.14	0.26
β_2	9.7	3.0	2.0
t_0 (ms)	5.60×10^{-3}	0.135	6.10
t_{tr} (ms)	6.10×10^{-3}	0.166	9.00
$t_{1/2}$ (ms)	6.30×10^{-3}	0.204	12.3
W	0.11	0.34	0.50

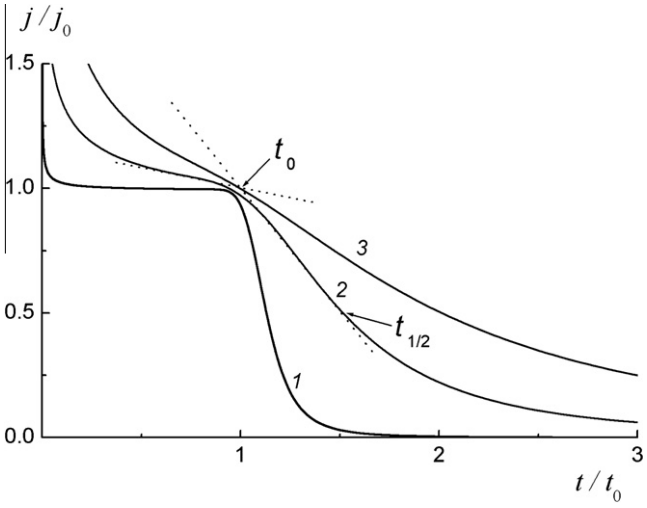

Fig. 2. The same transients as on Fig. 1 but in the linear normalized coordinates. The procedure to find t_0 and $t_{1/2}$ is shown for curve *2*.

(PF) effect. Instead, the dipolar disorder formalism introduces it in a prescribed manner contrary to the dipolar glass model, which explains this effect self-consistently [21,22]. It is not clear, which of the MTMg parameters fits best to account for the PF effect, if only in a prescribed manner. It seems to be the frequency factor v_0. Indeed, according to [12,22] the rate-limiting step in the dipolar glass model is the thermally activated release of carriers trapped by critical traps whose radius is effectively controlled by the applied electric field. Finally, we have

$$v_0 = k_{PF} v_{00}. \tag{2}$$

The factor k_{PF} is supposed to be close to the ratio of the carrier mobilities found at a given field strength F to that at $F \to 0$. In our analysis, k_{PF} is equal to this ratio taken from the published data for 30%DEH:PC [24]. The reported value of the PF slope $S = -\frac{d \lg \mu}{dF^{1/2}}$ is 0.39 $(\mu m/V)^{1/2}$.

Fig. 3 presents the computation results. TOF current transients are calculated with and without account of the PF effect. Also shown are equilibrium currents in a semi-infinite sample $(L \to \infty)$ given by dashed straight lines with primed numbers. As expected, only the field dependence of the steady-state currents (curve *1* on Fig. 4) strictly follows the PF law with the above indicated value of S (this dependence refers to the equilibrium mobility). We also processed the curves of Fig. 3 in linear coordinates and the resulting data for all three times of flight (t_{tr}, t_0 and $t_{1/2}$) are presented in Table 2 and Fig. 4.

According to the MTMg analysis [25], the equilibrium mobility $\tilde{\mu}$ in our case is equal to 8×10^{-6} $cm^2/V\,s$ and does not depend on the electric field. We equate it with the zero-field mobility $\mu(0)$ and use it as a standard in evaluating PF effect represented by the ratio $\mu/\mu(0)$ where μ stands for the mobility found using computed times of flight given in Table 2.

There are some problems with estimating data points for $F = 0$ for all curves except a theoretical one. Direct numerical computations for very small electric fields ($\leqslant$0.01 V/μm) are difficult to perform and besides, one has to take into account the presence of an ordinary diffusion (neglected so far). It is quite fair to assume that all zero-field mobilities are very close to $\mu(0)$.

It is seen that curves on Fig. 4 fall into two groups, one relating to PF effect (*1–4*) and the other (*5–7*) describing data for field independent frequency factor. In the first group, data based on $t_{1/2}$ best reproduces the PF theoretical dependence, followed by t_{tr} and t_0. But still, data scatter is not that conspicuous. We see that even for $v_0 = const$ the ratio $\mu/\mu(0)$ increases as the field rises, this fact being in line with the carrier transport becoming more and more dispersive. For completeness, we indicate the maximum values of this ratio at 200 V/μm: 508 (group 1) and 3.42 (group 2), respectively.

To judge the influence of the field on the current shape, we plotted normalized curves from Fig. 3 in linear coordinates as well (Fig. 5). Again, calculations include the case of no PF effect. The following observations should be noted.

At low fields (less than 20 V/μm) the PF effect is of almost no importance as far as the transient shape is concerned although the current shape itself changes dramatically (compare curves *6, 5*, and *4, 3*). In the absence of PF effect the transient shape changes continuously in the whole field range (as already reported in [9]), while PF curves practically do not change in the field range 20–200 V/μm, their transient shape acquiring an almost universal character. This behavior is reminiscent of the famous universality law found experimentally [18] and explained by the SM theory [18] or the MTM [26]. A weak universality found in the present work appears on $j - t$ plots and only in the time interval embracing the time of flight.

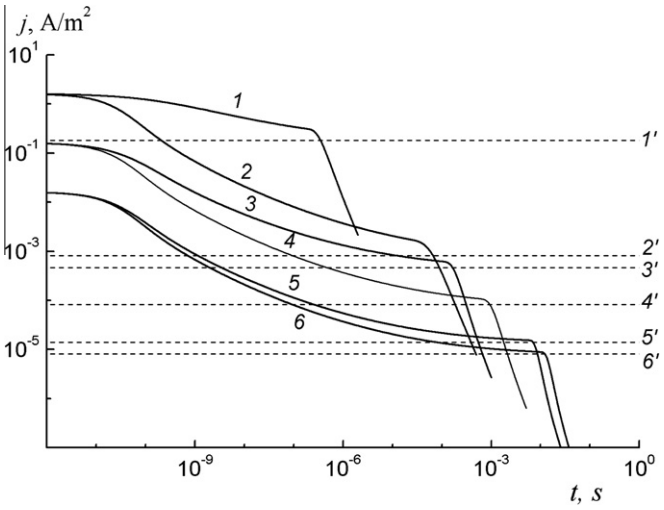

Fig. 3. Computed TOF transients (solid curves) in logarithmic coordinates with (*1, 3, 5*) and without (*2, 4, 6*) taking into account PF effect (see Table 2). Electric field 200 (*1, 2*), 20 (*3, 4*) and 2 V/μm (*5, 6*). Dashed straight lines refer to a semi-infinite sample and belong to the corresponding solid curve.

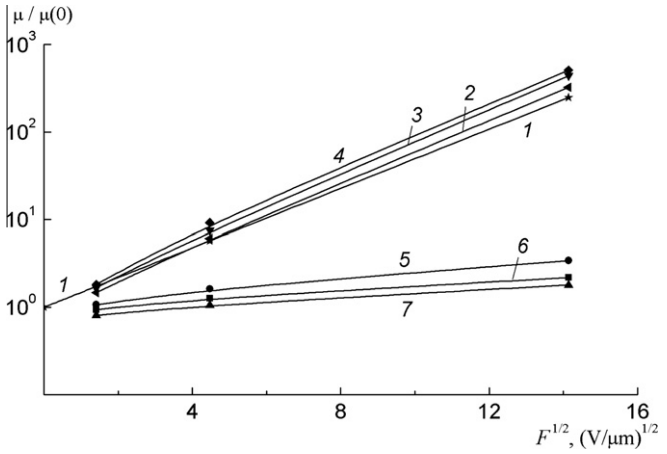

Fig. 4. Mobility ratio $\mu/\mu(0)$ as a function of the square root of the electric field. Theoretical curve *1* and the computed mobilities based on $t_{1/2}$ (*2, 7*), t_{tr} (*3, 6*) and t_0 (*4, 5*). PF effect taken into account (*1–4*) and neglected (*5–7*). The symbols are computed data points.

Table 2
Computed slopes and times of flight for three values of the electric field with and without account of the prescribed PF effect (see text).

Parameter	Field, V/μm					
	2		20		200	
PF factor	1	1.73	1	5.72	1	248
β_1	0.052	0.052	0.12	0.12	0.215	0.17
β_2	4.7	4.7	3.2	3.2	2.5	2.55
t_0 (ms)	11.7	6.86	0.77	0.136	36.5×10^{-3}	24.6×10^{-5}
t_{tr} (ms)	13.3	7.47	0.98	0.167	56.9×10^{-3}	28.4×10^{-5}
$t_{1/2}$ (ms)	15.4	8.78	1.18	0.205	69.3×10^{-3}	38.6×10^{-5}
W	0.22	0.24	0.35	0.37	0.47	0.36

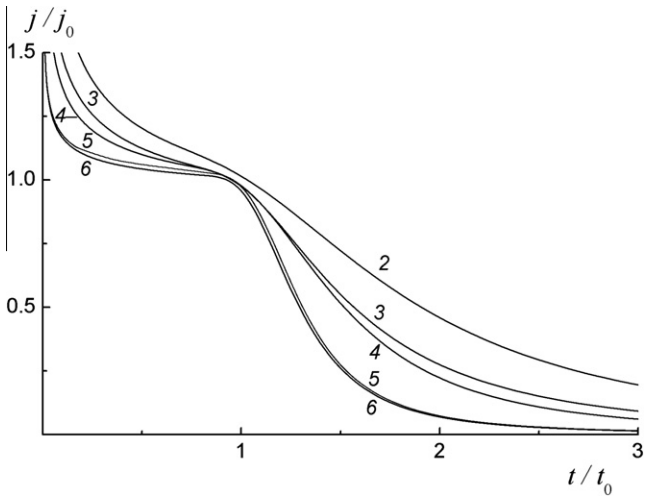

Fig. 5. Transients *2–6* from Fig. 3 presented in the linear normalized coordinates. j_0 –is the current density at the time of flight.

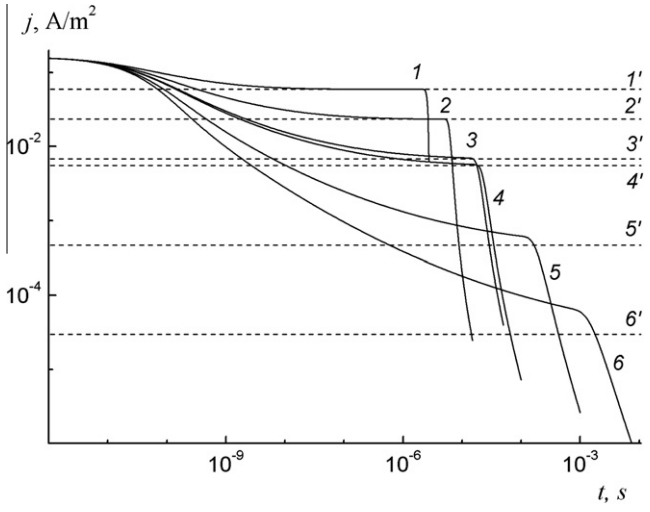

Fig. 6. Computed TOF transients (solid curves) in logarithmic coordinates referring to σ equal to 0.07 (*1–3*) and 0.1 eV (*4–6*) for temperatures 350 (*1, 4*), 290 (*2, 5*) and 250 K (*3, 6*). Dashed straight lines refer to a semi-infinite sample and belong to the corresponding solid curve.

At last, we performed numerical calculations of the mobility temperature dependence. Computed curves are presented in Fig. 6 for two values of σ (0.07 and 0.1 eV) and three temperatures (250, 290 and 350 K) with dashed straight lines referring again to a semi-infinite sample. Here we plot numerical data only for the case of $\nu_0 = const$ intending to explore mainly the effects of a non-equilibrium transport. The plots on Fig. 7 represent the temperature dependence of the transit times as a function of $1/T^2$.

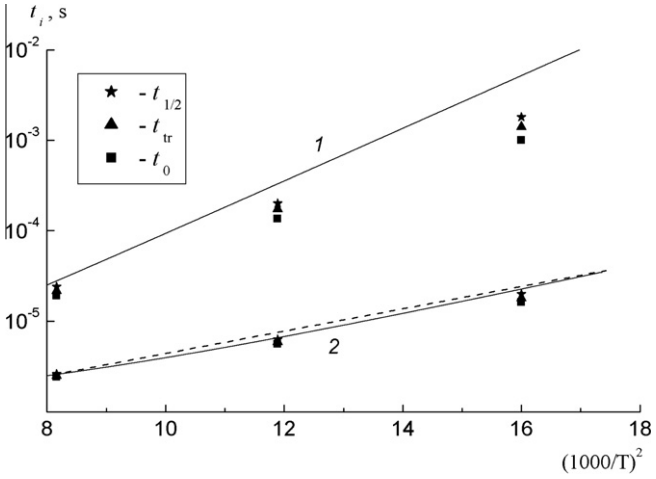

Fig. 7. Dependence of the times of flight on the inverse squared temperature.

Analytic formula [25] predicts that with a good approximation $\tilde{\mu}^{-1} \propto \exp\left(\frac{\sigma^2}{2k^2T^2}\right)$ which is slightly different from the famous GDM expression $\tilde{\mu}^{-1} \propto \exp\left(\frac{4\sigma^2}{9k^2T^2}\right)$ [7,8]. Our main interest is to check whether the general dependence $\ln \mu^{-1} \propto 1/T^2$ holds. One notes that for $\sigma = 0.07$ eV (*2*) even the theoretical curve shows some curvature but data points are very close to each other and to the theoretical curve. In the case of $\sigma = 0.1$ eV (*1*) the theoretical curve becomes straight but computed times of flight increasingly deviate from the theoretical dependence as temperature falls. As in the case of the PF effect, the least deviating data points belong to $t_{1/2}$ with those of t_0 deviating most. As a result, effective values of σ found from processing data for $t_{1/2}$, t_{tr} and t_0 are 0.084, 0.080 and 0.074 eV respectively compared to theoretical value 0.1 eV. We see that the effect of the non-equilibrium transport in this case is quite perceptible but for $\sigma = 0.07$ eV it is hardly seen.

3. Non-homogeneous polymer: two-layer model

Recently, we have shown that according to the GDM numerous examples of the flat plateaus on experimental TOF curves should not even appear [9]. In a similar situation, involving the weakly dispersive transport ($\alpha \approx 0.85$) one had to apply the two-layer multiple trapping model for universal current transients to describe successfully the experimental results obtained by a TOF-1a technique in 30%DEH:PC [12]. Let us try the same approach for the MTMg.

MTMg parameters describing the carrier transport reported in [11,12] have been slightly corrected to better fit the existing data cited in [24] so that $\sigma = 0.128$ eV, $\nu_0 = 1.25 \times 10^{11}$ s^{-1}, $\mu_0 = 0.01$ cm^2/V s, $\tau_0 = 2.4 \times 10^{-11}$ s. A defective layer 1 μm thick with inferior transport characteristics compared to the bulk has been introduced into the model (the sample thickness 13.8 μm, the electric field 20 V/μm).

Unlike [12], we propose to explain the origin of the surface defective layer as arising from the sublimation of the dopant molecules through the free surface exposed to air during coating/drying procedure. In electron-beam experiments reported in [11,12] it is this free side of the samples that invariably faced the beam. As a result, a thin depletion layer with a reduced concentration of the dopant has been controlling TOF transients. Due to an exponential concentration dependence, the carrier mobility in the depletion layer will be lower than in the bulk. Thus, there is no need to

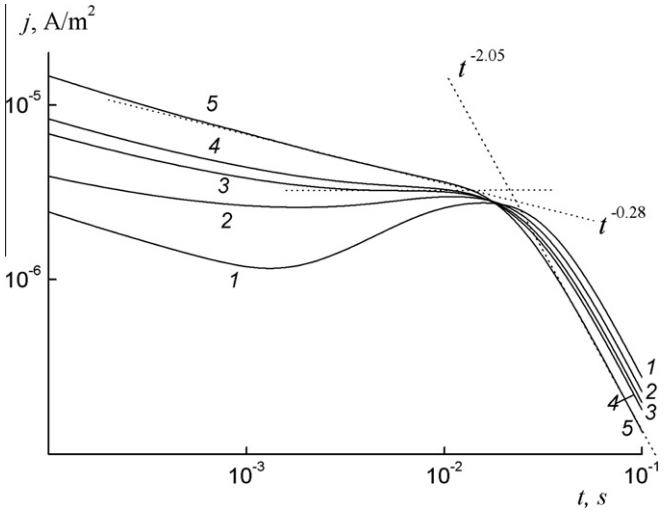

Fig. 8. Computed TOF-1a transients for a two-layer model in logarithmic coordinates. The thickness of the generation zone 1 (*1*), 1.5 (*2*), 2 (*3*), 2.4 μm (*4*) and the case of a homogeneous generation (*5*). Electric field 20 V/μm.

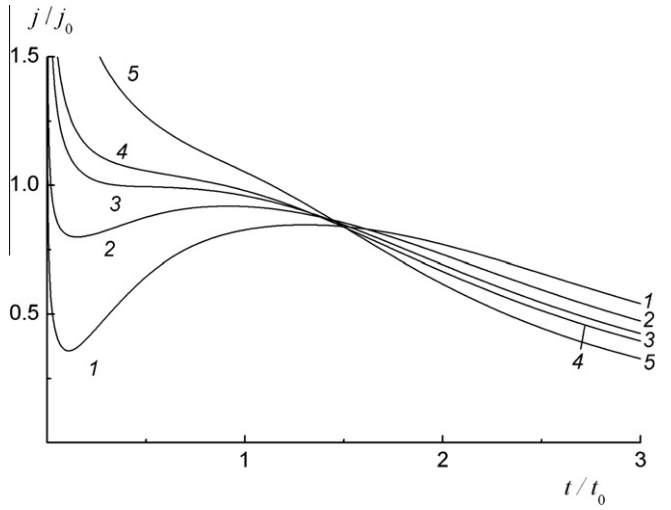

Fig. 9. The same transients as on Fig. 8 but in the linear normalized coordinates (all curves are normalized on t_0 and j_0 of curve *3*).

invoke any extrinsic traps. Also, it is only natural to expect that the Gaussian trap distribution should be the same in both parts of the sample with σ = 0.128 eV. Lowering μ_0 by a factor of six and applying Eqs. 1 and 2, we specify MTMg parameters for the depletion layer. Besides, the problem of an energetic set-off between the discreet transport level and the center of the trap distribution inherent in the approach adopted in [12] is automatically eliminated.

Computation results show (Figs. 8 and 9) that increasing the thickness of an irradiation zone (assumed rectangular like in [12]) causes the form of a "shoulder" marking the carrier transit across the sample to change continuously from a distinct cusp (curves *1* and *2*) through an outright flat (curve *3*) and a sloping plateau (curve *4*) to an almost featureless curve *5* for the case of the uniform irradiation.

Note the striking similarity in the shape variation found here and reported in [12]. It follows that the MTMg predicts appearance of flat plateaus even for the non-equilibrium regime (according to calculations $\beta_1 = 0.28$ and $\beta_2 = 2.05$ for a uniform excitation (TOF-2 experiment and curve *5* on Fig. 8 and 9) but only if a two-layer approach is involved. There are some fine distinctions between present results and those reported in [12].

The main difference concerns the shape of the TOF-2 current transients. In the latter case, the curve is truly featureless (as the experimental one) while curve *5* on Fig. 9 can be even processed on a linear $j - t$ plot, producing a transit time very close to that relating to a flat plateau. In addition, W values for flat plateaus do slightly differ (0.51 and 0.59 respectively).

4. Discussion

There are three experimental observations, which are central for an understanding of the carrier transport in MDPs. These are: (1) the electric field dependence of the mobility, (2) the temperature dependence of the mobility and (3) the transient current shape, which is used to determine the mobility [27].

According to [28]: "In their present form, existing models including Gaussian transport, field diffusion, Coulomb repulsion, intrinsic shallow trap controlled mobility, the Gaussian Disorder Model, Correlated Disorder Models, polaron theory, and Scher–Montroll theory, are unable to account for all the experimentally observed features of charge carrier transport in disordered systems".

In this situation, we extended the recently proposed two-layer MTM by replacing an exponential trap distribution with the Gaussian one, thus directly incorporating two most important physical characteristics of a real hopping process into the model. These are the total disorder energy σ as a parameter of the trap energy distribution and the zero-field mobility in the limit $T \to \infty$ as a quasi-band mobility μ_0. As a result, the model captures truthfully the non-Arrhenius mobility temperature dependence and the exponential mobility dependence on the average spacing between the dopants molecules as well. Again, the presence of σ comprised of the van-der-Waals and the dipolar disorder energies as given by the dipolar glass theory [21–23] allows one to accommodate the strong polarity effects encountered in experiment [4].

As for the current shape, the two-layer MTMg retains the ability of its predecessor (two-layer MTM [12]) to describe the whole sequence of TOF-1a curves encountered in experiment (initial spike, cusp, flat plateau, sloping shoulder, featureless curve) as the generation zone gets progressively wider with the rising electron beam energy.

The most intricate question concerns the ubiquitous Poole–Frenkel mobility field dependence. It has been demonstrated that its physical origin comes from the dipolar energy landscape, which happens to be spatially closely correlated [21–23]. The net effect of the spatial energy correlation consists in that the thermally activated release of holes trapped by critical traps whose radius becomes effectively controlled by the applied electric field [22]. It seems sound to suggest that exactly the frequency factor ν_0 should be ascribed the specified field dependence, if only in a prescribed manner at this stage.

Thus, the proposed two-layer MTMg seems to be capable of describing the non-equilibrium bulk carrier transport under uniform excitation (TOF-2 experiment) and explain the appearance of a flat plateau with anomalously broad tail at some intermediate electron energy (TOF-1a experiment), which generally should not be identified with the equilibration of the carrier transport. Even more, the new model is capable of accommodating both the non-Arrhenius mobility temperature dependence as well as its Poole–Frenkel field dependence. As an analytical model, it is amenable to accurate numerical calculations, which are not as time consuming as the Monte-Carlo simulations.

At the request of Referee, we now compare our calculations with the relevant Monte-Carlo simulations reported in [29,30] for a homogeneous system. It should be noted that those simulations

referred to a model organic semiconductor (ρ = 0.6 nm like in polyvinylcarbazole) for a range of σ (in particular, σ/kT) and studied the non-dispersive to dispersive transition. Unfortunately, simulation results were presented in arbitrary units only. Therefore, we could not draw any quantitative comparisons. Still, some qualitative comparisons are worth mentioning. Comparing Fig. 1 in our work and in [29] shows that β_1 rises with increasing σ quite similarly in both cases. Addressing Fig. 7 in [29], we see that curves presented on both linear and logarithmic plots resemble very closely our curve 3 on Figs. 1 and 2 (β_1 equals 0.27 and 0.26 eV respectively). The similarity increases even more if t-coordinate on our Fig. 2 is properly compressed. Thus, our numerical calculations qualitatively agree with the model Monte-Carlo simulations reported in [29,30].

5. Summary

We have shown that MTMg can successfully predict current shapes provided that GDM parameters are determined within the dipolar disorder formalism. Computations prove that the carrier transport is surely non-equilibrium for MDPs with $\sigma \geqslant 0.09$ at room temperature. The flat plateaus on TOF transients originate from the surface layer interference. For $\sigma \leqslant 0.075$ eV the theory predicts transport equilibration at typical experimental conditions ($T \geqslant 250$ K). All three times of flight ($t_{1/2}$, t_{tr} and t_0) are quite representative as far as the field and temperature dependence of the mobility is concerned, the second one being of universal application.

It is important that the proposed MTMg reproduces quite truthfully both the non-Arrhenius temperature mobility dependence as well as its ubiquitous PF field dependence. The first property is a direct consequence of the model parameter σ combining the van-der-Waals and the dipolar disorder energies. While the second one arises from the PF type field dependence of the model frequency factor prescribed by the dipolar glass model [21–23].

A two-layer extension of MTMg along the lines of the two-layer MTM recently suggested in [12] describes adequately TOF-1a results including flat plateau formation for the non-equilibrium carrier transport.

References

[1] A.B. Walker, A. Kambili, S.J. Martin, J. Phys.: Condens. Matter 14 (2002) 9825.
[2] G. Paasch, Th. Linder, C. Rost-Bietsch, S. Karl, W. Riess, S. Scheinert, J. Appl. Phys. 98 (2005). 084505..
[3] J.-L. Bredas, J.E. Norton, J. Cornil, V. Coropceanu, Acc. Chem. Res. 42 (2009) 1691.
[4] P.M. Borsenberger., D.S. Weiss Organic Photoreceptors. Marcel Dekker: New York. 1998.
[5] D.S. Weiss, M.A. Abkowitz, Chem. Rev. 110 (2010) 479.
[6] H. Bässler, A. Köhler, Top. Curr. Chem. 312 (2012) 1.
[7] H. Bässler, Phys. Stat. Sol. (b) 107 (1981) 9.
[8] H. Bässler, Phys. Stat. Sol. (b) 175 (1993) 15.
[9] A.P. Tyutnev, R.Sh. Ikhsanov, V.S. Saenko, E.D. Pozhidaev, J. Phys.: Condens. Matter 23 (2011) 325105.
[10] A.P. Tyutnev, R.Sh. Ikhsanov, V.S. Saenko, E.D. Pozhidaev, Electrochemistry. 48 (2012) 189.
[11] A.P. Tyutnev, V.S. Saenko, E.D. Pozhidaev, Kolesnikov V.A., J. Phys.: Condens. Matter 21 (2009) 115107.
[12] D.H. Dunlap, L.B. Schein, A.P. Tyutnev, V.S. Saenko, E.D. Pozhidaev, P.E. Parris, D.S. Weiss, J. Phys. Chem. C 114 (2010) 9076.
[13] L.B. Schein, Phil. Mag. B 65 (1992) 795.
[14] A.P. Tyutnev, V.S. Saenko, E.D. Pozhidaev, R.Sh. Ikhsanov, J. Phys.: Condens. Matter 20 (2008) 215219.
[15] P.M. Borsenberger, H. Bässler, J. Chem. Phys. 95 (1991) 5327.
[16] L. Pautmeier, R. Richert, H. Bässler, Phil. Mag. Lett. 59 (1989) 325.
[17] A.P. Tyutnev, V.S. Saenko, E.D. Pozhidaev, Chem. Phys. 389 (2011) 75.
[18] H. Scher, E.W. Montroll, Phys. Rev. B. 12 (1975) 2455.
[19] P.M. Borsenberger, L. Pautmeier, H. Bässler, J. Chem, Phys. 94 (1991) 5447.
[20] P.M. Borsenberger, E.H. Magin, J.J. Fitzgerald, J. Phys. Chem. 97 (1993) 9213.
[21] S.V. Novikov, D.H. Dunlap, V.M. Kenkre, P.E. Parris, A.V. Vannikov, Phys. Rev. Lett. 81 (1998) 4472.
[22] D.H. Dunlap, V.M. Kenkre, P.E. Parris, J. Imaging Sci, Technol. 43 (1999) 437.
[23] S.V. Novikov, A.V. Vannikov, J. Phys. Chem. C 113 (2009) 2532.
[24] L.B. Schein, V.S. Saenko, E.D. Pozhidaev, A.P. Tyutnev, D.S. Weiss, J. Phys. Chem. C 113 (2009) 1067.
[25] A.I. Rudenko, V.I. Arkhipov, Phil. Mag. B. 45 (1982) 177.
[26] V.I. Arkhipov, A.I. Rudenko, Phil. Mag. B. 45 (1982) 189.
[27] L.B. Schein, Russian J. Electrochemistry 48 (2012) 281.
[28] L.B. Schein, D.S. Weiss, D.H. Dunlap, A.P. Tyutnev, P.E. Parris, NIP 27 and Digital Fabrication. (2011) 304.
[29] P.M. Borsenberger, L.T. Pautmeier, H. Bässler, Phys. Rev. B. 46 (1992) 12145.
[30] P.M. Borsenberger, R. Richert, H. Bässler, Phys. Rev. B. 47 (1993) 4289.